J Solid State Electrochem (2011) 15:189–196
DOI 10.1007/s10008-010-1093-x

ORIGINAL PAPER

Evaluation of manganese and oxygen content in $La_{0.7}Sr_{0.3}MnO_{3-\delta}$ and correlation with the thermodynamic data

Speranta Tanasescu · Cornelia Marinescu · Florentina Maxim · Ancuta Sofronia · Nicolae Totir

Received: 26 August 2009 / Revised: 30 April 2010 / Accepted: 4 May 2010 / Published online: 18 May 2010

Abstract In order to understand how the thermodynamic properties are related to the oxygen and manganese content in the Sr-doped lanthanum manganites, nonstoichiometric perovskite phases $La_{0.7}Sr_{0.3}MnO_{3-\delta}$ have been investigated by using solid state electrochemical techniques, as well as wet chemical methods. The influence of the oxygen stoichiometry change on the thermodynamic properties was examined using the data obtained by a coulometric titration technique coupled with solid state electromotive force measurements (EMF). The results were correlated with the average Mn valence values as determined by a chemical method based on two independent iodometric titrations, with amperometric dead-stop end point detection. New features related to the relationship between the average Mn valence, the oxygen nonstoichiometry variation, and the thermodynamic behavior were evidenced.

Keywords Coulometric titration · Iodometric titration · Thermodynamic properties · Nonstoichiometry · Perovskites

Introduction

Among the perovskite-structured oxides, the lanthanum-strontium-manganese oxides are receiving considerable attention due to their wide-ranging electrical, magnetic, and catalytic properties. Replacement of trivalent lanthanum ions by divalent strontium ions leads to the formation of acceptors and the charge neutrality is maintained by a change in the valence state of the manganese ions and the formation of oxygen vacancies. The oxidation states are populated in various proportions depending on temperature, partial pressure of oxygen and Sr-doping [1–7]. These oxides may show a high electronic conductivity due to the mixed valence state and high oxide ion conductivity due to the high oxygen vacancy concentration. The knowledge of both the actual Mn oxidation state and the oxygen nonstoichiometry of the sample become then necessary, not only for an accurate characterization of the materials, but also for a correct interpretation of the physical properties. In the case of Sr-doped manganites (LSM), the interest relates both to high as well as low-temperature properties. LSM is widely used as cathode material in SOFCs. An increase in oxygen vacancy concentration with polarization of an LSM-cathode appears to be responsible for the improved performance of the cathodes material with increasing cathodic overpotential [7–9]. For the oxygen diffusion and the oxygen reduction kinetics on Sr-doped manganites, the oxygen vacancy concentration is of vital importance. The low temperature magnetic properties of LSM's also vary with the oxygen stoichiometry of the material, which has been equilibrated at high temperature [10–13]. The colossal magnetoresistive (CMR) properties may entirely be determined by the valence conversion between Mn^{3+} and Mn^{4+}, and thus, the creation of oxygen vacancies could reduce the double exchange effect, resulting in a decrease in the CMR effect [13].

In practice, however, quantifying of oxygen vacancies is still a challenge. X-ray and neutron diffuse scattering can be used to determine vacancies in large bulk single crystalline specimens. Although some defect models have been proposed to explain the defect structure of the doped $LaMnO_3$ oxides, there are still controversies in the application of the defect structure models and the quantitative defect concentration calculations are rather scarce [2–4, 14–16]. Besides, the

S. Tanasescu (✉) · C. Marinescu · F. Maxim · A. Sofronia · N. Totir
Institute of Physical Chemistry "Ilie Murgulescu",
Splaiul Independentei 202,
060021 Bucharest, Romania
e-mail: stanasescu2004@yahoo.com

defects concentration in A-site acceptor doped ABO_3 perovskites is in turn a function not only of the composition but equally importantly the thermal history of the phase. Consequently, an understanding of the high temperature defect chemistry of phases is vital, if an understanding of the low temperature electronic and magnetic properties is to be achieved. At this point, investigations from thermodynamic point of view are very important. Moreover, few experimental data are available in the literature [5, 16–18].

In order to obtain further insight into physical mechanisms explaining the properties of the Sr-doped lanthanum manganites, in the present paper combined iodometric titration, EMF and solid state coulometric titration experiments were performed and the composite data were analyzed to make clear the relationship between the average Mn valence, the oxygen nonstoichiometry variation, and the thermodynamic behaviour of $La_{0.7}Sr_{0.3}MnO_{3-\delta}$ nonstoichiometric compositions with δ values comprised between 0.019 and 0.053.

Materials and methods

Samples

The powder of the $La_{0.7}Sr_{0.3}MnO_3$ specimens was supplied by Haldor Topsøe A/S, Lyngby, Denmark. These were prepared by drip pyrolysis and the phase content (X-ray powder diffraction), specific area, carbon content, and elemental compositions were checked on the processed powders [19]. After calcination at 1,173 K for 2 h, the powders showed a single-phase perovskite-type XRD pattern. For EMF and solid state coulometric titration measurements, the samples are made by pressing the powders into small pellets (2 mm thick and 2 mm high) weighing 40 mg and sintering at 1,273 K in air for 4 h.

EMF and solid-state coulometric titration measurements

The solid-oxide electrolyte electrochemical cells method was employed to obtain the thermodynamic properties of the samples. For combined EMF and solid-state coulometric titration measurements, a three-electrode cell was used. The cell consists of three electrodes (the sample and two iron-wüstite electrodes) embedded in a small disc of 12.84 wt.% yttria stabilized zirconia. One of the iron-wüstite electrode was used as a reference, to record the electromotive force, while the other was used as a counter, to titrate oxygen. The experimental method and apparatus were previously described [5]. Their principal characteristics are the following:

- The geometry of the three electrode work cell ensures a compact electrode–electrolyte assembly, so that temperature uniformity is easily reached and the extraneous thermoelectric potentials are minimized.
- The insulation of the electrodes in compartments which are separately evacuated and monitored for the gas pressure provides an adequate solution to remove the oxygen transfer between the electrodes through the gas and to prevent the extraneous electrode–gas interactions.
- The cell assembly is inserted into a system of protective quartz tubes between which vacuum is produced, in order to avoid air penetration through quartz, into the installation, at high temperatures (above 1,173 K). The measurements were carried out at a residual gas pressure of 10^{-5}–10^{-6} Pa, after a previous rinsing of the installation with purified argon.
- Prevention of signal pick-up from external heating sources is achieved by the use of a non-inductive furnace and by the adequate shielding of cell and leads.

The normal procedures in the EMF and coulometric titration experiments were as follows:

The electromotive force measurements were performed in the 1,073 to 1,273 K temperature range by using a Keithley 2000 Multimeter. The EMF was measured at 50 K intervals, each time waiting until equilibrium values are recorded. The determinations were considered as being satisfactory when EMF values for increasing and decreasing temperature agreed within 1 or 2 mV.

The free energy change of the cell when the intensive properties are kept constant is given by the expression:

$$\Delta G_{\text{cell}} = \mu_{O_2} - \mu_{O_{2(\text{ref})}} = 4FE \tag{1}$$

where E is the steady state EMF of the cell in volts; μ_{O_2}, $\mu_{O_{2(\text{ref})}}$ are respectively, the oxygen chemical potentials of the sample and the reference electrode and F is the Faraday constant (F=96.508 kJ/V equiv.).

By using the experimental values of the electromotive force of the cell and knowing the free energy change of the reference electrode [20–22], the values of the relative partial molar free energy of the solution of oxygen in the perovskite phase and hence the pressures of oxygen in equilibrium with the solid can be calculated:

$$\Delta \overline{G}_{O2} = RT \ln p_{O_2} \tag{2}$$

The relative partial molar enthalpies and entropies were obtained according to the known relationships [5]:

$$\frac{\partial \frac{\Delta \overline{G}_{O_2}}{T}}{\partial T} = -\frac{\Delta \overline{H}_{O_2}}{T^2} \tag{3}$$

$$\Delta \overline{G}_{O_2} = \Delta \overline{H}_{O_2} - T\Delta \overline{S}_{O_2} \tag{4}$$

The overall uncertainty due to the temperature and potential measurement (taking into account the overall uncertainty of a single measurement and also the quoted

accuracy of the voltmeter) was ±1.5 mV. This was equivalent to ±0.579 kJ mol^{-1} for the free energy change of the cell. Considering the uncertainty ±0.523 kJ mol^{-1} in the thermodynamic data for the iron-wüstite references [20–22], the overall accuracy of the data was estimated to be 1.6 kJ mol^{-1}. For the enthalpies the errors were ±0.45 kJ mol^{-1} and for the entropies ±1.1 J mol^{-1} K^{-1}. Errors due to the data taken from the literature are not included in these values because of the unavailability of reliable standard deviations.

After the steady state measurements were completed over a range of temperatures, at a constant composition, oxygen was removed from the sample by isothermal solid state coulometric titration [5, 23]. The titrations were performed in situ at 1,123 K by using a Bi-PAD Tacussel Potentiostat. A constant current (I) is passed through the cell for a predetermined time (t). Because the transference number of the oxygen ions in the electrolyte is unity, the time integral of the current is a precise measure of the change in the oxygen content [5, 23–25]. The equivalents of charge passed ($I\,t$) are related to the moles of the oxygen leaving the electrode. According to Faraday's law, the mass change $|\Delta m|$ (g) of the sample is related to the transferred charge Q (A·s) by:

$$|\Delta m| = 8.291 \cdot 10^{-5} Q \tag{5}$$

As one can see, a charge of $1 \cdot 10^{-5}$ A s, which is easily measurable corresponds to a weight change of only 8×10^{-10} g. This makes it possible to achieve extremely high compositional resolution, and very small stoichiometric widths can be investigated.

After the desired amount of electricity was passed through the cell, the current circuit was opened and sufficient time (about 3 h) had to be allowed for the electrode to equilibrate. Practically, we considered that EMF had reached its equilibrium value when three subsequent readings at 30 min intervals varied by less than 0.5 mV. After the sample reached equilibrium, for every newly obtained composition, the temperature was changed under open-circuit condition, and the equilibrium EMFs for different temperatures between 1,073 and 1,273 K were recorded.

Measurements of the manganese concentration and manganese average oxidation state by iodometry

A classical method for the Mn valence determination by measurement of chlorine evolved when compounds are dissolved in hydrochloric acid was firstly described by Jonker and Wan Santen [10]. Because the manganese and the oxygen content per unit formula remain undetermined, this method does not permit the evaluation of the compound stoichiometry. To define such parameters it is in fact necessary to measure both, the total amount of Mn and the average Mn valence. Iodometric method described by Vogel [26] and improved by Licci et al. [27] is based on two independent iodometric titration, carried out under controlled conditions, which make it possible to separately determine the total amount of Mn, and the equivalent Mn charge; the average Mn valence is represented by the ratio between these two quantities. Considering this method as most suitable to obtain information about the valence state of manganese ions, we used the same concept in our investigation on Sr-doped lanthanum manganites. The home-made iodometric titration equipment set-up in our laboratory is presented in Fig. 1. The installation is under continuum flow of Ar in order to avoid any trace of oxygen. Titration cell has a 250 ml capacity and was equipped with multi-hole lid, from which the electrodes, the reagents and the gas stream were introduced. For the amperometric titration a double Pt electrode (103 mm long, Radiometer Analytical, France) was used.

The first iodometric titration run (run A) is used for the obtaining of total equivalents of Mn. A known quantity of the powdered sample (M_A) was dissolved in dilute H_2SO_4, in presence of 5–10 drops of H_2O_2. The obtained solution was diluted to a fixed volume after the excess of H_2O_2 was completely boiled off. A measured fraction of the solution was treated with an excess of sodium bismuthate which, at room temperature oxidized Mn^{2+} to Mn^{7+}. The unreacted bismuthate was filtered and the solid residue was washed with diluted nitric acid. The filtered liquid was transferred in the titration cell and fluxed with Ar for 15 min; an excess of KI was added. The equivalent volume, V_A was obtained by immediately titration of liberated I_2 with thiosulphate solution. In the evaluation of the average valence of Mn it is not necessary to standardize the thiosulphate solution because in the two independent titrations the same solution is used. Considering only the active species, V_A corresponds to total equivalents of Mn for the redox process, according to the reaction:

$$Mn^{7+} + 5I^- \rightarrow Mn^{2+} + 5/2 I_2 \tag{6}$$

In the second titration experiment (run B), the Mn oxidation equivalents have been measured. A new quantity of the grounded sample (M_B) was weighed directly in the titration cell; it fluxed with Ar for 15 min. Oxygen-free KI solution and diluted HCl solution were added in sequence. Perovskite instantaneously dissolved and I_2 developed, according to the reaction:

$$Mn^{(2+n)+} + nI^- \rightarrow Mn^{2+} + n/2 I_2 \tag{7}$$

The liberated I_2 was immediately titrated with the same thiosulphate solution used in the run A and the equivalent titrant volume, V_B, was determinate.

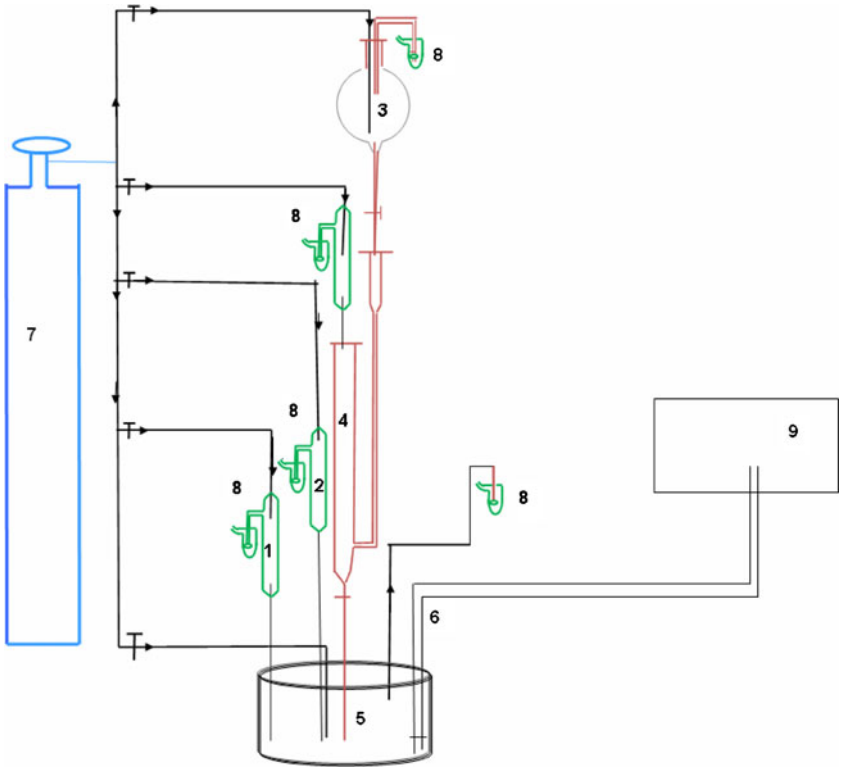

Fig. 1 The scheme of the equipment used for iodometric titration: *1*, *2* reagents holder; *3* thiosulphate holder; *4* burette; *5* titration cell; *6* Pt double electrode; *7* argon tank; *8* argon exit; *9* potentiostat

If it is denoted $I_{ox}=V_A/M_A'$ and $I_{red}=V_B/M_B$, from Eqs. 2 and 3 one can obtain [27]

$$5I_{red}/I_{ox}=n \tag{8}$$

where n represents the average Mn charge exceeding 2, and $(2+n)$ is the average valence of manganese in the compound. To simplify we will note the average valence of manganese with $<Mn>_{vs}$.

Experimental procedure to obtain composite data

In order to make the correlation of the results obtained from solid state electromotive force (EMF) measurements and solid state coulometric titration experiments with the ratio of manganese ions calculated from redox titration, the measurements were performed according to the following procedure: (a) iodometric titration at room temperature to determine the average manganese ions before the EMF and coulometric titration; (b) EMF measurements in the temperature range of 1,073–1,273 K (at rinsing and descending the temperature) in order to determine (before the change in situ of the oxygen stoichiometry) the partial molar thermodynamic data of oxygen dissolution in the perovskite phase and the equilibrium partial pressure of oxygen; (c) in situ isothermal solid state coulometric titration in order to perform a particular change of nonstoichiometry in controlled conditions; (d) EMF measurements in the temperature range of 1,073–1,273 K (at rinsing and descending the temperature) after the in situ change of the stoichiometry in order to determine for the new nonstoichiometric composition the partial molar thermodynamic data of oxygen dissolution in the perovskite phase and the equilibrium partial pressure of oxygen; e) slowly cooling the sample in situ (no more than 5 °C per hour) until room temperature; e) iodometric titration at room temperature for the new composition to determine the average manganese ions.

Determining the ratio of manganese ions for every nonstoichiometric sample before and after the EMF and solid state coulometric titration experiments will allow: (1) to verify if every change in situ of the oxygen stoichiometry could be indeed correlated with the change of the average manganese ions measured at room temperature by iodometric titration; (2) to verify the type of correlation between the average manganese ions and the oxygen content for $La_{0.7}Sr_{0.3}MnO_{3-\delta}$ in the investigated domain of nonstoichiometry; (3) to evidence the effect of manganese and oxygen content on the thermodynamic data of $La_{0.7}Sr_{0.3}MnO_{3-\delta}$. All these results are particularly important for the LSM high, as well as lower temperature applications.

It is noticed that all the measurements performed on a sample during the (b, c, d) runs were registered keeping all the time the sample in situ.

Results and discussion

Emphasizing the role of charge ordering in explaining the magneto transport properties of the manganites, Jonker and

Table 1 Results of the coulometric titration and iodometric analysis obtained for $La_{0.7}Sr_{0.3}MnO_{3-\delta}$ with different oxygen content

Composition of samples (by coulometric titration)	Composition of samples (by iodometry)	Charge introduced by Mn valence conversion (calculated)	Charge due to the oxygen vacancy (calculated)
$La_{0.7}Sr_{0.3}MnO_{2.981}$	$La_{0.7}Sr_{0.3}MnO_{2.982}$	0.264^{+}	0.036^{-}
$La_{0.7}Sr_{0.3}MnO_{2.967}$	$La_{0.7}Sr_{0.3}MnO_{2.966}$	0.232^{+}	0.068^{-}
$La_{0.7}Sr_{0.3}MnO_{2.956}$	$La_{0.7}Sr_{0.3}MnO_{2.955}$	0.21^{+}	0.092^{-}
$La_{0.7}Sr_{0.3}MnO_{2.947}$	$La_{0.7}Sr_{0.3}MnO_{2.948}$	0.196^{+}	0.104^{-}

van Santen [10] considered that the local charge in the doped manganites is balanced by the conversion of Mn valence between Mn^{3+} and Mn^{4+} and the creation of oxygen vacancies, as well. Consequently, the proposed ionic structure of $La_{1-x}A_xMnO_{3-\delta}$ is:

$$La^{3+}_{1-x}A^{2+}_{x}Mn^{3+}_{1-x+2\delta}Mn^{4+}_{x-2\delta}O^{2-}_{3-\delta}V^{0}_{\delta} \quad (9)$$

where V^0_δ stands for the fraction of oxygen vacancies. From (9), the mean valence state of Mn is:

$$Mn_{vs} = 3 + x - 2\delta \quad (10)$$

where x=0.3. The $<Mn>_{vs}$ is determined from iodometric titration measurements, as previously described. Therefore, the content of oxygen vacancies δ can be calculated and the charge introduced by Mn valence conversion, as well as the charge due to the oxygen vacancy could be evaluated. The average reproducibility error of δ determination by iodometry was found to be ±0.005. The calculated values are shown in the Table 1.

The composition of samples with δ calculated from iodometry confirms the nonstoichiometry of the samples imposed by coulometric titration (Table 1). The calculated values of the oxygen content are consistent with that obtained by coulometry, a maximum $\Delta\delta$=±0.001 being observed between the values obtained by the two methods. The results show the decreasing of the Mn^{4+} concentration and the increasing of the charge due to the oxygen vacancy. Thus in the case of $La_{0.7}Sr_{0.3}MnO_{2.982}$, 88% of the residual charge introduced by Sr doping is balanced by the conversion of Mn^{3+} to Mn^{4+} and 12% by oxygen vacancies. Instead, for $La_{0.7}Sr_{0.3}MnO_{2.955}$, 70% of the residual charge is balanced by the conversion of manganese valence and 30% by oxygen vacancies. Because the Mn^{4+}/Mn^{3+} ratio is related to the chemical potential term, its contribution is considered to be weighted by the concentration of the related defects. To further evaluate these results, the thermodynamic data could give a valuable help.

The representative results concerning the variations of the partial molar thermodynamic data with the temperature and oxygen stoichiometry in the oxygen deficient region are depicted in Figs. 2 and 3. $\Delta\overline{G}_{O_2}$ decreases with the oxygen nonstoichiometry. At the same deviation of oxygen stoichiometry, the energy values increase with temperature, suggesting the increasing of the oxygen vacancies concentration. The plots of $\Delta\overline{G}_{O_2}$ versus T form straight lines. From the slopes of the plots, $\Delta\overline{H}_{O_2}$ and $\Delta\overline{S}_{O_2}$ were calculated and the results are shown in Fig. 3 as a function of δ. In this figure, the average valence number of manganese ions corresponding to δ is shown on the upper scale. The highest values of the enthalpies and entropies are obtained for a small departure from stoichiometry. Between δ=0.019 and δ=0.046, both the values of enthalpy and entropy decrease remarkably with δ, suggesting the change of the predominant defects and the increase in the binding energy of oxygen. From δ=0.046 to δ=0.053, both $\Delta\overline{H}_{O_2}$ and $\Delta\overline{S}_{O_2}$ increase again, the variations of the entropies values indicating the change of order in the oxygen sublattice.

Let us consider the oxygen incorporation reaction given by the equation:

$$O_2{}^{gas} + 2\{V_{\ddot{o}}\} + 4e' \leftrightarrow \text{nil} \quad (11)$$

where e' is an electron in a partially filled wide band, and the lattice oxygen vacancies are assumed to be randomly distributed and noninteracting [28]. Because changes of oxygen concentration result in changes of mean oxide ion vacancy concentration and of mean Mn valence, $\Delta\overline{S}_{O_2}$ includes the partial molar entropy of the configurational

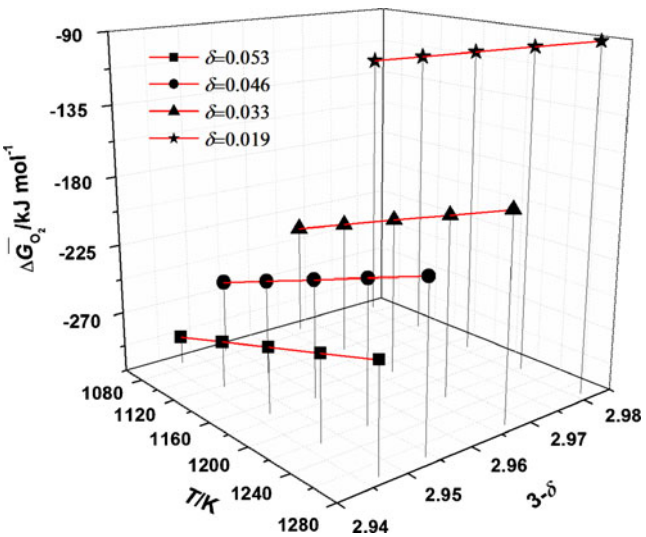

Fig. 2 $\Delta\overline{G}_{O_2}$ variation with the temperature and oxygen non-stoichiometry for $La_{0.7}Sr_{0.3}MnO_{3-\delta}$

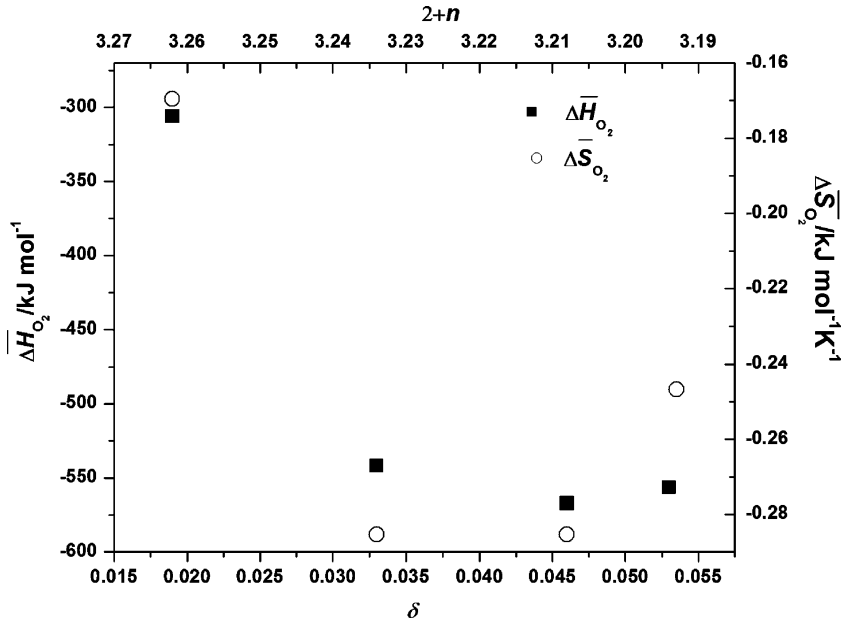

Fig. 3 Variation of the $\Delta\overline{H}_{O_2}$ and $\Delta\overline{S}_{O_2}$ with oxygen stoichiometry change and average manganese valence

entropy change of oxygen lattice sites, S_O (config), and the entropy change of the delocalized electronic state. The oxygen partial molar entropy due to configuration of vacancy on the sublattice is expressed by [28, 29]:

$$S_O(\text{config}) = R\ln[\delta/(3-\delta)] \quad (12)$$

Neglecting vibrational effects, the difference $\Delta\overline{S}_{O_2} - 2S_O(\text{config}) = \Delta S^0$ is an entropy term that is independent of δ. Most of the large negative value of ΔS^0 is due to the entropy of O_2 (g), $\Delta S^0{}_{O_2}$, which is about 251 $J\cdot mol^{-1}\cdot K^{-1}$ in the temperature range 1,073–1,173 K [30]. The other contribution to ΔS^0 noted as $\Delta S^0{}_1 = \Delta S^0 - \Delta S^0{}_{O_2}$, represents the standard entropy change in the oxide caused by the reaction (11). Due to the large decrease in $\Delta\overline{S}_{O_2}$ obtained with the stoichiometry change for LSM with small departure to stoichiometry, it is considered that the oxygen vacancies would not randomly distribute on all of the oxygen sites but they would be distributed to some particular oxygen sites. This result agrees with the data obtained by Mizusaki and coworkers from temperature gravimetry on $La_{0.6}Sr_{0.4}MnO_{3-\delta}$ [18]. As suggested, it is also possible that the vacancy distribution is related to some crystallographic distortions or ordering of metal sites [18]. Instead, for higher departure from stoichiometry, higher values of $\Delta\overline{S}_{O_2}$ are obtained after titration. It is expected that the change in $\Delta\overline{S}_{O_2}$ with δ in this case to be essentially determined by the change in S_O (config) and, therefore, the oxygen vacancies randomly distribute on the oxygen sites. Presently, however, further details and measurements of the energy and entropy of oxygen incorporation into LSM at different values of nonstoichiometry δ are necessary in order to make clear the vacancy distribution with the stoichiometry change.

Considering the partial pressure of oxygen as a key parameter for the thermodynamic characterization of the materials, we investigated the variation of the $logp_{O_2}$ data with the temperature and the average manganese valence of the nonstoichiometric compositions (Fig. 4). In the figure, the lines are guide for eyes. One can observe that the $logp_{O_2}$ shifted to higher values with increasing temperature. For the compound with small departure from stoichiometry (δ= 0.019), higher p_{O_2} values than those generally attributed to the oxygen-deficient nonstoichiometry are obtained with increasing temperature. This discrepancy was also observed by Mizusaki et al. [2, 18]. In spite of this discrepancy, the conductivity data [2] show that the nonstoichiometry is still oxygen deficient type. At the same temperature, $logp_{O_2}$

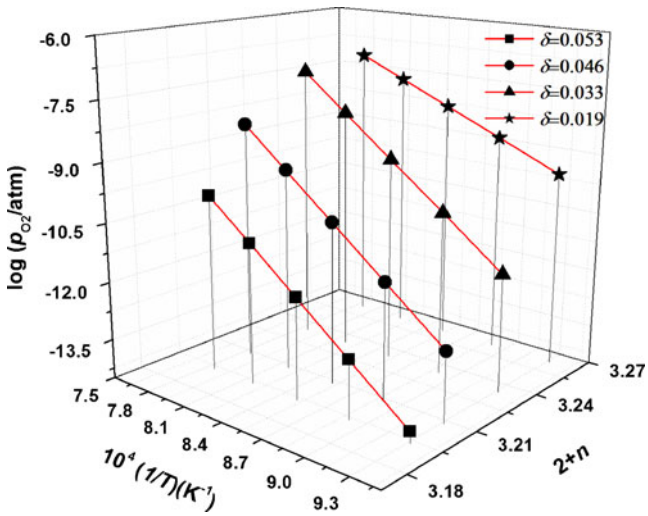

Fig. 4 The oxygen partial pressure variation with the temperature and average valence of manganese ions

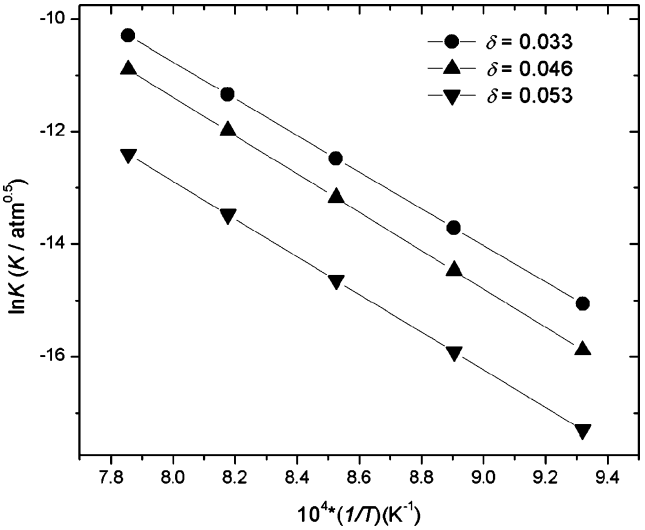

Fig. 5 Plot of ln$K$ versus $1/T$

values increase with the increasing in the average valence of manganese ions. This observation is consistent with the experimental results indicated by Mizusaki et al. [6] for a larger domain of nonstoichimetry in $La_{1-x}Sr_xMnO_{3-\delta}$ with $x \geq 0.3$.

Considering that in the oxygen-deficient region the nonstoichiometry is essentially determined by the random distribution of oxygen vacancies, a correlation between the defect equilibrium and the experimental data obtained in this work is discussed in the following. According to random-defect model previously described [2, 4, 6], the formation of oxygen vacancies is accompanied by the reduction of two M^{4+}-ions to two M^{3+}-ions, or in Kröger-Vink notation [31]:

$$2Mn^{\cdot}{}_{Mn} + O_O^x \leftrightarrow 2Mn^{x}{}_{Mn} + V_O^{\bullet\bullet} + 0.5O_2 \quad (13)$$

The relationship between δ and p_{O_2} [4] is then described by:

$$K = \frac{\delta(1 - x + 2\delta)p_{O_2}^{0.5}}{(3-\delta)\cdot(x-2\delta)^2} \quad (14)$$

In order to verify the model we calculated the equilibrium constants from our experimental results at δ=0.033; 0.046; 0.053 (Fig. 5). They were found to increase with increasing temperature, which suggests that at higher temperatures the defect reaction proceed in the direction of formation of a significant amount of oxygen vacancies. Comparing these values with the lines calculated according to this defect model, we obtained a good agreement. From the plots of the equilibrium constants as a function of $1/T$, the thermodynamic properties of defect formation can be obtained. Enthalpy and entropy terms determined in this manner, in the temperature range of 1,073–1,273 K, are shown in Table 2. They are in good agreement with the values calculated by Nowotny and Rekas [4] according to the random-defect model. The difference between the data is mostly a consequence of the difference in the Sr concentration, as well as in the temperature range in which they are valid.

The combined analysis of the thermodynamic data with the results obtained by both solid state coulometric titration and iodometric titration methods attest the decreasing of the Mn^{4+} concentration and the increasing of the charge due to the oxygen vacancy when δ changes from 0.019 to 0.053. At the same time, the method we describe attest that the solid state coulometric titration is an effective method to obtain nonstoichiometric composition and that the high temperature thermodynamic data obtained for the compounds in situ could be used to explain the critical dependence of the physical properties on the oxygen stoichiometry.

Conclusions

The nonstoichiometry in the oxygen-deficient $La_{0.7}Sr_{0.3}MnO_{3-\delta}$ was examined by correlating the results regarding the oxygen and manganese content obtained by solid state coulometric titration and iodometric titration methods, with the thermodynamic data of the oxygen dissolution in the perovskite phase. The combined analysis of the results allows determining the role played by oxygen vacancies in balancing the local charge in LSM. The data show that the remarkable thermodynamic properties of the investigated samples could be explained not only qualitatively by the structural changes upon doping, but also by the fact that the thermodynamics is extremely sensitive to the chemical defects in oxygen sites. The correlation between the defect equilibrium and the experimental data obtained in this work attests that the nonstoichiometry in the oxygen-deficient La(Sr)$MnO_{3-\delta}$ is essentially determined by the random distribution of oxygen vacancies.

Bearing in mind the role of charge ordering and of the defects chemistry in explaining the electrical, magnetic and

Table 2 The thermodynamic properties of defect formation according to the reaction (13)

Strontium content, x, in $La_{1-x}Sr_xMnO_{3-\delta}$	Temperature range (K)	ΔH^0 (kJ mol^{-1})	ΔS^0 (J mol^{-1} K^{-1})	Ref.
0.3	1,073–1,373	283.6±1.2	132.2±1.1	This study
0.2	1,273–1,473	302.5±15.3	114.5.5±11.7	Nowotny J et al.[4]

thermodynamic behaviour of the doped lanthanum manganites, it should be possible to find new routes for modifying the properties of these materials by controlling the Mn^{3+}/Mn^{4+} ratio and creating vacancies in the oxygen sites.

Acknowledgment We wish to thank Risø National Laboratory-Denmark for supplying the solid electrolyte used in EMF measurements for thermodynamic investigations.

This paper has been prepared in the frame of the PN–II–ID–PCE Project no. 50/2007 under financial support from the Romanian Ministry of Research and Education (ANCS).

References

1. Kuo JH, Anderson HU, Sparlin DM (1990) J Solid State Chem 87:55–63
2. Mizusaki J (1992) Solid State Ionics 52:79–91
3. Roosmalen JAM, Cordfunke EHP (1994) J Solid State Chem 110:113–117
4. Nowotny J, Rekas M (1998) J Am Ceram Soc 81:67–80
5. Tanasescu S, Totir ND, Marchidan DI (1998) Electrochim Acta 43:1675–1681
6. Mizusaki J, Mori N, Takai H, Yonemura Y, Minamiue H, Tagawa H, Dokiya M, Inaba H, Naraya K, Sasamoto T, Hashimoto T (2000) Solid State Ionics 129:163–177
7. Fleig J (2003) Annu Rev Mater Res 33:361–382
8. Fleig J, Maier J (2004) J Eur Ceram Soc 24:1343–1347
9. Gauckler LJ, Beckel D, Buergler BE, Jud E, Muecke UR, Prestat M, Rupp JLM, Richter J (2004) Chimia 58:837–850
10. Jonker GH, Santen JH (1950) Physica XVI 3:337–349
11. De Teresa JM, Dorr K, Muller KH, Shultz L (1998) Phys Rev B 58:5928–5931
12. Abdelmoula N, Guidara K, Cheikh-Rouhou A, Dhahri E, Joubert JC (2000) J Solid State Chem 151:139–144
13. Tanasescu S, Grecu MN, Marinescu C, Giurgiu LM, Chiriac H, Urse M (2009) Adv Appl Ceram 108:273–279
14. Kofstad P, Petrov A (1993) On the defect structure and non-stoichiometry in doped perovskites: $La_{1-x}Sr_xMnO_{3\pm\delta}$. In: Poulsen FW et al (eds) Proc 14th Riso International Symposium on Material Science, Denmark, pp 287–296
15. Poulsen FW (2000) Solid State Ionics 129:145–162
16. Grundy AN, Hallstedt B, Gauckler LJ (2004) CALPHAD: Computer Coupling of Phase Diagrams and Thermochemistry 28:191–201
17. Kuo JH, Anderson HU, Sparlin DM (1989) J Solid State Chem 83:52–60
18. Mizusaki J, Tagawa H, Naraya K, Sasamoto T (1991) Solid State Ionics 49:111–118
19. Gordes P, Christiansen N (1994) Combustion synthesis of perovskite oxides used in SOFC technology. In: Bossel U (ed) Proc. 1st European SOFC Forum, PV 2. Lucerne, Switzerland, pp 567–575
20. Charette GG, Flengas SN (1968) J Electrochem Soc 8:796–804
21. Kelley KK (1960) U S Bur of Mines Bull 584
22. Kelley KK, King EG (1961) U S Bur of Mines Bull 592
23. Wagner C (1953) J Chem Phys 21:1819–1827
24. Weppner W, Chen L-C, Piekarczyk W (1980) Z Naturforsch 35a:381–388
25. Marchidan DI, Tanasescu S (1976) Rev Roum Chim 21:1451–1455
26. Vogel AI (1964) A text-book of quantitative inorganic analysis including elementary instrumental analysis. Longmans, London
27. Licci F, Turilli G, Ferro P (1996) J Magn Magn Mater 164:L268–L272
28. Lankhorst MHR, Bouwmeester HJM, Verweij H (1997) J Am Ceram Soc 80:2175–2198
29. Mizusaki J, Mima Y, Yamauchi S, Fueki K, Tagawa H (1989) J Solid State Chem 80:102–111
30. Stull DR, Prophet H (eds) (1971) ANAF thermochemical tables, 2nd edn. US Government Printing Office, National Bureau of Standards, Washington, D.C
31. Kröger FA, Vink HJ (1956) Relations between the concentrations of imperfections in crystalline solids. In: Seitz F, Turnball D (eds) Solid state physics, vol 3. Academic, New York, pp 310–438